Bonn Potential and Shell-Model Calculations for ^{206,205,204}Pb

L. Coraggio,[1,2] A. Covello,[1] A. Gargano,[1] N. Itaco,[1] and T. T. S. Kuo[2]
[1] *Dipartimento di Scienze Fisiche, Università di Napoli Federico II, and Istituto Nazionale di Fisica Nucleare, Complesso Universitario di Monte S. Angelo, Via Cintia - I-80126 Napoli, Italy*
[2] *Department of Physics, SUNY, Stony Brook, New York 11794*
(February 9, 2008)

The structure of the nuclei ^{206,205,204}Pb is studied in terms of shell model employing a realistic effective interaction derived from the Bonn A nucleon-nucleon potential. The energy spectra, binding energies and electromagnetic properties are calculated and compared with experiment. A very good overall agreement is obtained. This evidences the reliability of our realistic effective interaction and encourages use of modern realistic potentials in shell-model calculations for heavy-mass nuclei.

21.60.Cs,21.30.Fe,27.80.+w

The Pb isotopes have long been the subject of great experimental and theoretical interest. This is of course related to the fact that ^{208}Pb is a very good doubly magic nucleus, whose neighbors are accessible to a variety of spectroscopic studies. This is not the case for other nuclei in the vicinity of closed shells like the ^{100}Sn and ^{132}Sn neighbors. These nuclei, in fact, lie well away from the valley of stability and only recently our knowledge of their spectroscopic properties has significantly improved thanks to the advent of large multidetector γ-ray arrays.

From the theoretical point of view the study of nuclei with few valence particles or holes provides the best testing ground for the basic ingredients of shell-model calculations, especially as regards the matrix elements of the two-body residual interaction. In most of the several calculations performed so far in the lead region, phenomenological potentials have been used for the two-body interaction [1–3]. As early as some twenty-five years ago, however, a realistic effective interaction derived from the Hamada-Johnston nucleon-nucleon (NN) potential [4] was employed in the works of Refs. [5,6]. Since that time there has been much progress towards a microscopic approach to nuclear structure calculations starting from a free NN potential. On the one hand, the theoretical framework in which the model-space effective interaction $V_{\rm eff}$ can be derived from a given NN potential has been largely improved (the main aspects of this derivation are reviewed in Ref. [7]). On the other hand, high-quality NN potentials have been constructed which give an excellent description of the NN scattering data. Among these of special interest for microscopic nuclear structure work are those based on quantitative meson-theoretic models. A review of the major developments in this field is given in Ref. [8].

These improvements have opened the way to a new generation of realistic shell-model calculations which should assess to which extent modern realistic interactions can provide a consistent and accurate description of nuclear structure phenomena. Until now, however, attention has been focused on medium-mass nuclei, such as the Sn isotopes and the $N = 82$ isotones [9–14]. In our own studies [9–11] we considered the ^{100}Sn neighbors going from ^{102}Sn to ^{105}Sn while for the $N = 82$ isotones we were concerned with the ^{132}Sn neighbors with two and three valence protons. In both cases we performed shell-model calculations using a realistic effective interaction derived from the meson-theoretic Bonn A potential [15]. The very good agreement between theory and experiment achieved in these works makes apparent the motivation for the present study of the ^{206,205,204}Pb isotopes. These nuclei with two, three and four holes in the N=82-126 shell offer the opportunity to put to a test our realistic effective interaction in the A=208 region.

In this paper, we assume that ^{208}Pb is a closed core and let the valence neutron holes occupy the six single-hole (s.h.) orbits $2p_{1/2}$, $1f_{5/2}$, $2p_{3/2}$, $0i_{13/2}$, $1f_{7/2}$, and $0h_{9/2}$. As regards the energy spacings between the six s.h. levels, we take all of them from the experimental spectrum of ^{207}Pb [16]. They are (in MeV): $\epsilon_{f_{5/2}} - \epsilon_{p_{1/2}} = 0.570$, $\epsilon_{p_{3/2}} - \epsilon_{p_{1/2}} = 0.898$, $\epsilon_{i_{13/2}} - \epsilon_{p_{1/2}} = 1.633$, $\epsilon_{f_{7/2}} - \epsilon_{p_{1/2}} = 2.340$, and $\epsilon_{h_{9/2}} - \epsilon_{p_{1/2}} = 3.414$.

As in our prior work [9–11], we make use of two-body effective interaction derived from the Bonn A free NN potential. The main difference between the present and earlier calculations is that here we treat neutrons as valence holes, which implies the derivation of a hole-hole effective interaction. This was obtained using a G-matrix formalism, including renormalizations from both core polarization and folded diagrams. We have chosen the Pauli exclusion operator Q_2 in the G-matrix equation,

$$G(\omega) = V + VQ_2\frac{1}{\omega - Q_2TQ_2}Q_2G(\omega), \tag{1}$$

as specified [7] by $(n_1, n_2, n_3) = (22, 36, 66)$ for the neutron orbits and $(n_1, n_2, n_3) = (16, 28, 66)$ for the proton orbits. Here V represents the NN potential, T denotes the two-nucleon kinetic energy, and ω is the so-called starting

energy. We employ a matrix inversion method to calculate the above G matrix in an essentially exact way [17]. In the calculation of the effective interaction we take the so-called $\hat{Q}$-box [7] to be composed of G-matrix diagrams through second order in G. They are the seven first- and second-order diagrams considered in Ref. [18] with the particle lines replaced by hole lines. This brings about changes in the phase factors and off-shell energy variables. Since in ^{208}Pb neutrons and protons have different closed shell cores, $Z = 82$ and $N = 126$, respectively, in the calculation of $V_{\rm eff}$ we use an isospin uncoupled representation, where protons and neutrons are treated separately. For the shell-model oscillator $\hbar\omega$ we use the value 6.88 MeV, as obtained from the expression $\hbar\omega = 45A^{-\frac{1}{3}} - 25A^{-\frac{2}{3}}$ for A=208.

The experimental [19,20] and theoretical spectra of ^{206}Pb and ^{205}Pb are compared in Figs. 1 and 2, where we report all the calculated and experimental levels up to 2.5 and 1.5 MeV for the former and the latter, respectively. In the higher-energy region we only compare the calculated high-spin states with the observed ones. As regards ^{204}Pb, all experimental [21] and calculated levels up to 2.0 MeV are reported in Fig. 3 while high-spin states are shown in Fig. 4. From Figs. 1-3 we see that a very good agreement with experiment is obtained for the low-energy spectra. In particular, in each of the three nuclei the theoretical level density reproduces remarkably well the experimental one. Note too that each state of a given J^π in any of three calculated spectra has its experimental counterpart, with a few exceptions. In fact, as may be seen in Fig. 2, the $\frac{5}{2}^-$, $(\frac{3}{2},\frac{1}{2})^-$, and $(\frac{9}{2},\frac{7}{2})^-$ states observed at 1.265, 1.374 and 1.499 MeV in ^{205}Pb cannot be safely identified with levels predicted by the theory. As regards ^{204}Pb, we find the 0^+_4 state at 1.954 MeV while the experimental one, which is not reported in Fig. 3, lies at 2.433 MeV. It should be mentioned, however, that the theory predicts four more 0^+ states in the energy interval 2.2–2.6 MeV. Aside from these uncertainties, the agreement between calculated and experimental spectra is such as to allow us to identify experimental states with no firm or without spin-parity assignment. For ^{206}Pb our results suggest that the observed levels at 2.197 and 2.236 MeV have $J^\pi = 3^+$ and 1^+, respectively. As for ^{205}Pb, we predict $J^\pi = \frac{1}{2}^-$ and $\frac{3}{2}^-$ for the experimental levels at 0.803 an 0.998 MeV.

Regarding the quantitative agreement between our results and experiment, the discrepancy for the 2^+_1 states in ^{206}Pb and ^{204}Pb is only about 40 keV, while all other excited states in the low-energy spectra of both nuclei lie about 200 keV below the experimental ones. The rms deviation σ [22] is 207 and 216 keV for ^{206}Pb and ^{204}Pb, respectively. The agreement with experiment is even better for ^{205}Pb. In this case the σ value is 74 keV, excluding the three above mentioned states, for which we have not attempted any identification.

Concerning the high-spin states in ^{206}Pb and ^{205}Pb, from Figs. 1 and 2 we see that they are also well described by the theory. In ^{204}Pb the agreement between theory and experiment is rather worse for the states lying above 4.3 MeV excitation energy, the largest discrepancy being about 400 keV for the 16^+_2 state.

We have also calculated the ground-state binding energies (relative to ^{208}Pb). The mass excess value for ^{207}Pb needed for absolute scaling of the s.h. levels was taken from [26]. We find $E_b(^{206}\text{Pb})$=-14.240, $E_b(^{205}\text{Pb})$=-22.147, and $E_b(^{204}\text{Pb})$=-28.927 MeV, to be compared with the experimental values -14.106(6), -22.194(6), and -28.925(6) MeV [26], respectively.

Let us now come to the electromagnetic observables. Concerning the magnetic properties, we have specified the effective $M1$ operator in the following way. Five s.h. matrix elements have been determined from the measured magnetic moments and $M1$ transition rates in ^{207}Pb. The available experimental information regards the moments of the $\frac{1}{2}^-$, $\frac{5}{2}^-$, and $\frac{3}{2}^-$ states [23,24] and the $B(M1;\frac{3}{2}^- \rightarrow \frac{1}{2}^-)$ and $B(M1;\frac{3}{2}^- \rightarrow \frac{5}{2}^-)$ [16]. The effective $i_{13/2}$ $M1$ operator has been determined from the magnetic moment of the 12^+ state in ^{206}Pb which arises from the $(i_{13/2})^{-2}$ configuration. For the remaining matrix elements, we have used the bare operator quenched by the factor 0.6. In this way, the $M1$ operator was specified by nine s.h. matrix elements. In Table I we compare the experimental magnetic moments in ^{206,205,204}Pb [23] with the values calculated with both the bare operator and the effective $M1$ operator specified above. We see that the latter values are in very good agreement with experiment, most of them falling within the error bars. The only significant discrepancy is the sign of the magnetic moment of the 6^- state in ^{206}Pb. It should be noted that this disagreement was also found in Ref. [6], where the difficulty to understand the measured positive value is evidenced. We fully agree with the conclusion of the above work and think that a new measurement of this magnetic moment is most desirable. It is worth mentioning that, as can be easily verified from Table I, no state-independent quenching of the bare operator can lead to a satisfactory agreement. Only one $B(M1)$ value is known. This is the $B(M1;6^- \rightarrow 7^-)$ in ^{206}Pb which has been measured to be 0.045(13) W.u. [16]. Our calculated value is 0.132 W.u.

As regards the calculation of the $E\lambda$ observables, we have used an effective neutron hole charge $e_n^{\rm eff} = 0.82e$. This has been obtained from the observed $B(E2;\frac{5}{2}^- \rightarrow \frac{1}{2}^-)$ in ^{207}Pb [16]. In Tables II and III we compare the calculated quadrupole moments and $E\lambda$ transition rates with the experimental ones [23,19,20,25,21]. Generally, the agreement is very good, the main discrepancy regarding the sign of the quadrupole moment of the 2^+ state in ^{204}Pb.

In summary, we have presented here the results of a shell-model study of the neutron hole isotopes ^{206,205,204}Pb, where use has been made of an effective two-hole interaction derived from the Bonn A nucleon-nucleon potential. We have shown that a large number of experimental data regarding the three nuclei considered are very well reproduced

by the theory. It should be emphasized that these are the first shell-model calculations for heavy-mass nuclei in which the effective interaction is derived from a modern NN potential by means of a G-matrix folded diagram method. In fact, as already mentioned, the earlier realistic calculation of Ref. [6] made use of an effective interaction derived from the Hamada-Johnston potential and including only the bare interaction and the core polarization (or bubble) diagram. In addition, to obtain good agreement with experiment, the bubble diagram matrix elements were multiplied by the single empirical constant 0.75. The same effective interaction has been recently used [27] to describe the results of a detailed experimental study of ^{206}Pb via the ^{205}Pb(n,γ) reaction.

We may conclude that our present results, which are quite consistent with those obtained for nuclei around ^{100}Sn and ^{132}Sn, provide further insight into the role of modern realistic interactions in nuclear structure calculations, evidencing, in particular, the merit of the Bonn potential.

ACKNOWLEDGMENTS

This work was supported in part by the Italian Ministero dell'Università e della Ricerca Scientifica e Tecnologica (MURST) and by the U.S. DOE Grant No. DE-FG02-88ER40388. One of us (L.C.) wishes to acknowledge the hospitality received while at SUNY and also thank the Angelo Della Riccia Foundation for financial support.

---

[1] See Ref. 6 for a comprehensive list of references through 1973.
[2] D. Wang and M. T. McEllistrem, Phys. Rev. C **42**, 252 (1990), and references therein.
[3] C. A. P. Ceneviva, L. Losano, N. Teruya, and H. Dias, Nucl. Phys. **A619**, 129 (1997), and references therein.
[4] T. Hamada and I. D. Johnston, Nucl. Phys. **34**, 382 (1962).
[5] G. H. Herling and T. T. S. Kuo, Nucl. Phys. **A181**, 113 (1972).
[6] J. B. McGrory and T. T. S. Kuo, Nucl. Phys. **A247**, 283 (1975).
[7] T. T. S. Kuo, in *New Perspectives in Nuclear Structure*, Proceedings of the Fifth International Spring Seminar on Nuclear Physics, Ravello, 1995, edited by A. Covello (World Scientific, Singapore, 1996), p. 159.
[8] R. Machleidt and G. Q. Li, Phys. Rep. **242**, 5 (1994).
[9] F. Andreozzi, L. Coraggio, A. Covello, A.Gargano, T. T. S. Kuo, Z. B. Li, and A. Porrino, Phys. Rev. C **54**, 1636 (1996).
[10] F. Andreozzi, L. Coraggio, A. Covello, A. Gargano, T. T. S. Kuo, and A. Porrino, Phys. Rev. C **56**, R16 (1997).
[11] A. Covello, F. Andreozzi, L. Coraggio, A. Gargano, T. T. S. Kuo, and A. Porrino, Prog. Part. Nucl. Phys. **38**, 165 (1997).
[12] A. Holt, T. Engeland, E. Osnes, M. Hjorth-Jensen, and J. Suhonen, Nucl. Phys. **A618**, 107 (1997).
[13] J. Suhonen, J. Toivanen, A. Holt, T. Engeland, E. Osnes, and M. Hjorth-Jensen, Nucl. Phys. **A628**, 41 (1998).
[14] A. Holt, T. Engeland, M. Hjorth-Jensen, and E. Osnes, Nucl. Phys. **A634**, 41 (1998).
[15] R. Machleidt, K. Holinde, and Ch. Elster, Phys. Rep. **149**, 1 (1987).
[16] M. J. Martin, Nucl. Data Sheets **70**, 313 (1993).
[17] E. M. Krenciglowa, C. L. Kung, T. T. S. Kuo, and E. Osnes, Ann. Phys. (N.Y.) **101**, 154 (1976).
[18] J. Shurpin, D. Strottman, and T. T. S. Kuo, Nucl. Phys. A **408**, 310 (1983).
[19] R. G. Helmer and M. A. Lee, Nucl. Data Sheets **61**, 93 (1990).
[20] S. Rab, Nucl. Data Sheets **69**, 679 (1993).
[21] M. R. Schmorak, Nucl. Data Sheets **72**, 409 (1994).
[22] We define $\sigma = \{(1/N_d)\sum_i [E_{\rm expt}(i) - E_{\rm calc}(i)]^2\}^{\frac{1}{2}}$, where N_d is the number of data.
[23] P. Raghavan, At. Data Nucl. Data Tables **42**, 189 (1989).
[24] H. V. Kapdor, P. von Brentano, E. Grosse, and K. Haberkant, Nucl. Phys. **A152**, 263 (1970).
[25] C. G. Lindén, I. Bergström, J. Blomqvist, K.-G. Rensfelt, H. Sergolle, and K. Westerberg, Z. Phys. A **277**, 273 (1976).
[26] G. Audi and A. H. Wapstra, Nucl. Phys. **A565**, 1 (1993).
[27] S. Raman, J. B. McGrory, E. T. Jurney, and J. W. Starner, Phys. Rev. C **53**, 2732 (1996).

FIG. 1. Experimental and calculated spectrum of ^{206}Pb.

FIG. 2. Experimental and calculated spectrum of ^{205}Pb.

FIG. 3. Experimental and calculated low-energy spectrum of ^{204}Pb.

FIG. 4. Experimental and calculated high-spin states in ^{204}Pb.

TABLE I. Calculated and experimental magnetic moments (in n.m.) in ^{206,205,204}Pb. The theoretical values have been obtained by using (a) an effective $M1$ operator (se text for details), and (b) the free $M1$ operator.

Nucleus	J^π	μ		
		Expt.	Calc.(a)	Calc.(b)
^{206}Pb	2_1^+	≤ 0.030	0.057	0.340
	7_1^-	-0.1519 (28)	-0.277	-0.736
	6_1^-	0.78 (42)	-1.20	-2.02
	12_1^+	-1.795 (22)	-1.794	-3.532
^{205}Pb	$(\frac{5}{2}^-)_1$	0.7117 (4)	0.695	1.185
	$(\frac{13}{2}^+)_1$	-0.975 (40)	-0.897	-1.794
	$(\frac{25}{2}^-)_1$	-0.845 (14)	-1.010	-2.564
	$(\frac{33}{2}^+)_1$	-2.442 (83)	-2.467	-4.856
^{204}Pb	2_1^+	< 0.02	0.04	0.30
	4_1^+	0.225 (4)	0.306	0.856

TABLE II. Calculated and experimental electric quadrupole moments (eb) in ^{206,205,204}Pb.

Nucleus	J^π	Q	
		Expt.	Calc.
^{206}Pb	2_1^+	0.05 (9)	0.26
	7_1^-	0.33 (5)	0.37
	12_1^+	0.51 (2)	0.46
^{205}Pb	$(\frac{5}{2}^-)_1$	0.226 (37)	0.164
	$(\frac{13}{2}^+)_1$	0.30 (5)	0.35
	$(\frac{25}{2}^-)_1$	0.63 (3)	0.55
^{204}Pb	2_1^+	0.23 (9)	-0.11
	4_1^+	0.44 (2)	0.32

TABLE III. Calculated and experimental $B(E\lambda)$ (in W.u.) in ^{206,205,204}Pb.

Nucleus	$J_i^\pi \rightarrow J_f^\pi$	λ	B(Eλ)	
			Expt.	Calc.
^{206}Pb	$2_1^+ \rightarrow 0_1^+$	2	2.85 (3)	2.64
	$6_1^- \rightarrow 7_1^-$	2	≤ 0.4	0.05
	$7_1^- \rightarrow 4_2^+$	3	0.28 (4)	0.11
	$7_1^- \rightarrow 4_1^+$	3	0.36 (6)	0.21
^{205}Pb	$(\frac{25}{2}^-)_1 \rightarrow (\frac{21}{2}^-)_1$	2	0.62 (2)	0.60
	$(\frac{33}{2}^+)_1 \rightarrow (\frac{29}{2}^+)_1$	2	0.63 (21)	0.60
	$(\frac{13}{2}^+)_1 \rightarrow (\frac{7}{2}^-)_1$	3	0.00198 (22)	0.0002
	$(\frac{25}{2}^-)_1 \rightarrow (\frac{19}{2}^+)_1$	3	0.088 (8)	0.008
	$(\frac{33}{2}^+)_1 \rightarrow (\frac{27}{2}^-)_1$	3	0.15 (3)	0.01
	$(\frac{33}{2}^+)_1 \rightarrow (\frac{29}{2}^-)_1$	3	0.17 (2)	0.01
^{204}Pb	$2_1^+ \rightarrow 0_1^+$	2	4.65 (6)	3.28
	$4_1^+ \rightarrow 2_1^+$	2	0.00382 (14)	0.08
	$0_2^+ \rightarrow 2_1^+$	2	≤ 0.80	0.01
	$4_1^+ \rightarrow 0_1^+$	4	2.5 (5)	3.3

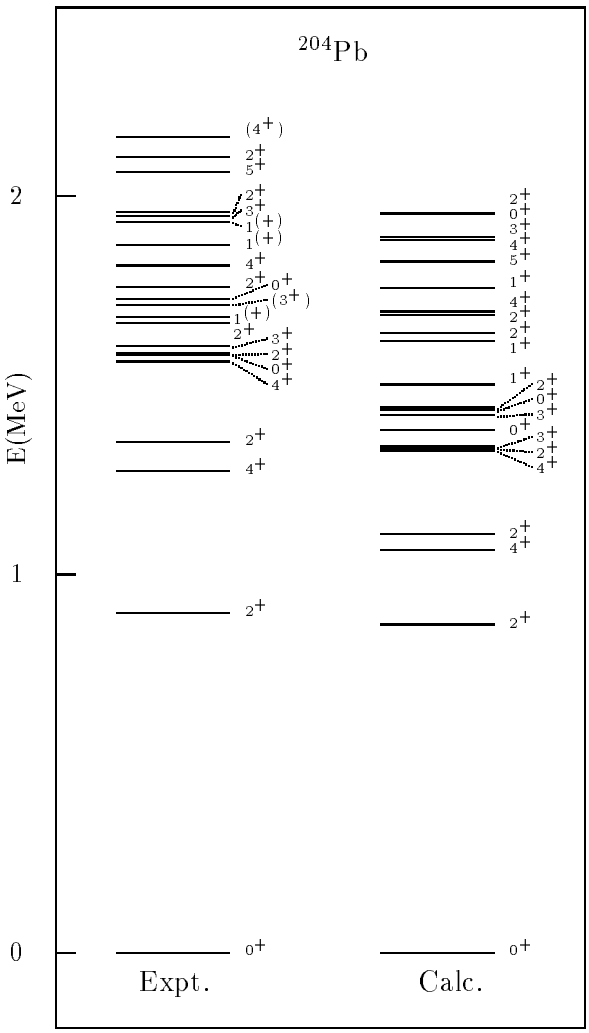
^{204}Pb
E(MeV)
2
1
0
(4^+)
2^+
5^+
2^+
3^+
$1^{(+)}$
$1^{(+)}$
4^+
2^+
0^+
(3^+)
$1^{(+)}$
2^+
3^+
2^+
0^+
4^+
2^+
4^+
2^+
0^+
Expt.
2^+
0^+
3^+
4^+
5^+
1^+
4^+
2^+
2^+
1^+
1^+
2^+
0^+
3^+
0^+
3^+
2^+
4^+
2^+
4^+
2^+
0^+
Calc.

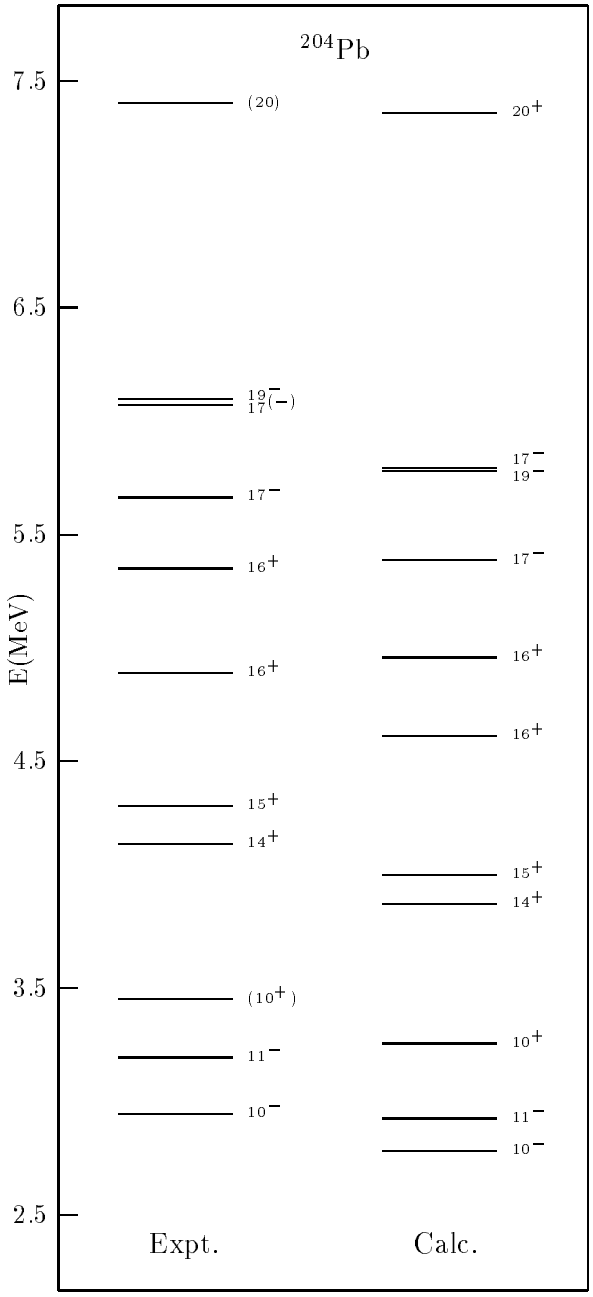
^{204}Pb
7.5
6.5
5.5
4.5
3.5
2.5
E(MeV)
(20)
19^-
$17^{(-)}$
17^-
16^+
16^+
15^+
14^+
(10^+)
11^-
10^-
20^+
17^-
19^-
17^-
16^+
16^+
15^+
14^+
10^+
11^-
10^-
Expt.
Calc.

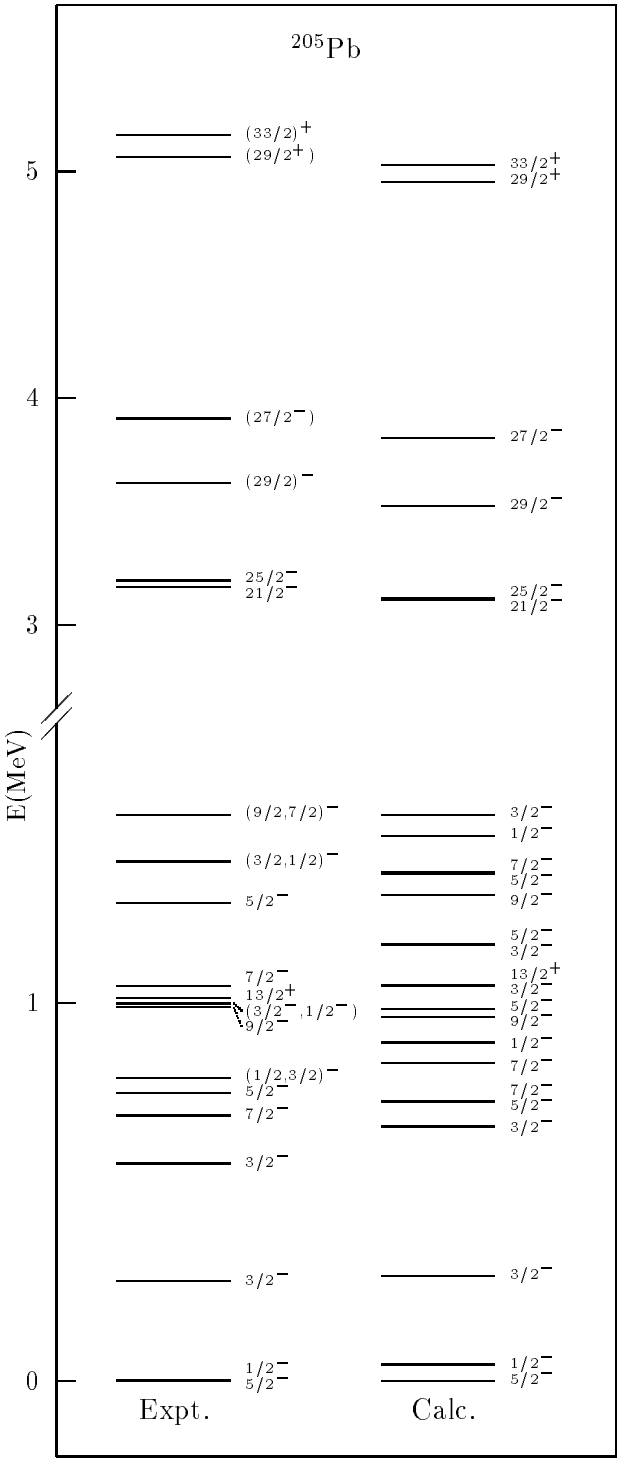
^{205}Pb
E(MeV)
5
4
3
1
0
$(33/2)^+$
$(29/2^+)$
$(27/2^-)$
$(29/2)^-$
$25/2^-$
$21/2^-$
$(9/2,7/2)^-$
$(3/2,1/2)^-$
$5/2^-$
$7/2^-$
$13/2^+$
$(3/2^-,1/2^-)$
$9/2^-$
$(1/2,3/2)^-$
$5/2^-$
$7/2^-$
$3/2^-$
$3/2^-$
$1/2^-$
$5/2^-$
Expt.
$33/2^+$
$29/2^+$
$27/2^-$
$29/2^-$
$25/2^-$
$21/2^-$
$3/2^-$
$1/2^-$
$7/2^-$
$5/2^-$
$9/2^-$
$5/2^-$
$3/2^-$
$13/2^+$
$3/2^-$
$5/2^-$
$9/2^-$
$1/2^-$
$7/2^-$
$7/2^-$
$5/2^-$
$3/2^-$
$3/2^-$
$1/2^-$
$5/2^-$
Calc.

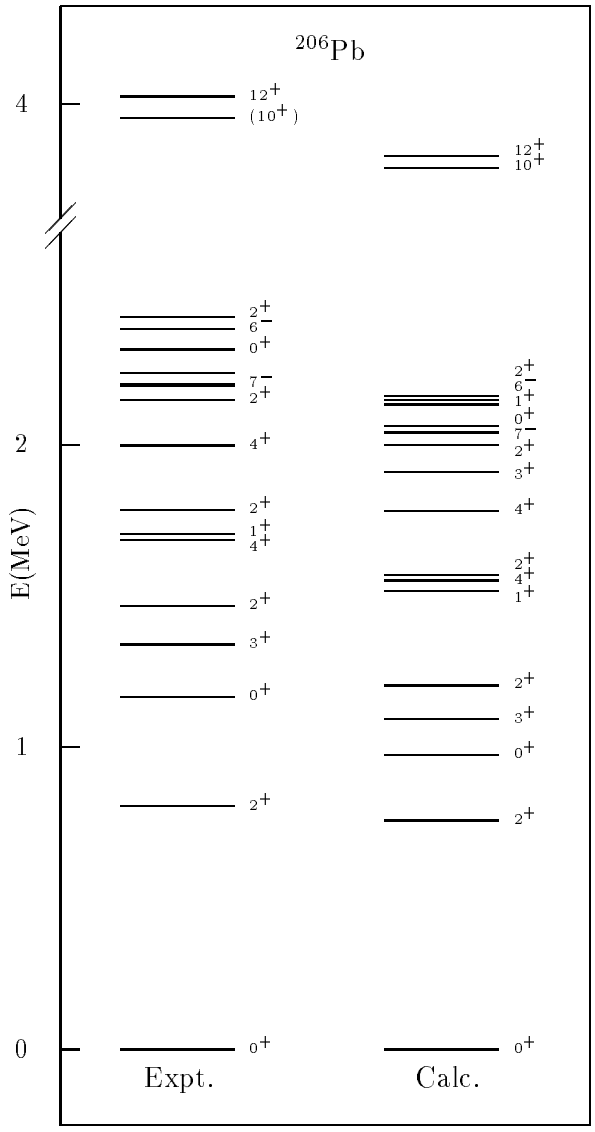
^{206}Pb
E(MeV)
4
2
1
0
12^+
(10^+)
2^+
6^-
0^+
7^-
2^+
4^+
2^+
1^+
4^+
2^+
3^+
0^+
2^+
0^+
Expt.
12^+
10^+
2^+
6^-
1^+
0^+
7^-
2^+
3^+
4^+
2^+
4^+
1^+
2^+
3^+
0^+
2^+
0^+
Calc.